The American Journal of Pathology, Vol. 193, No. 6, June 2023

ELSEVIER

The American Journal of
PATHOLOGY
ajp.amjpathol.org

MUSCULOSKELETAL PATHOLOGY

Investigating Eukaryotic Elongation Factor 2 Kinase/Eukaryotic Translation Elongation Factor 2 Pathway Regulation and Its Role in Protein Synthesis Impairment during Disuse-Induced Skeletal Muscle Atrophy

Natalia Vilchinskaya,* Wooi Fang Lim,[†‡§] Svetlana Belova,* Thomas C. Roberts,[†‡§] Matthew J.A. Wood,[†‡§] and Yulia Lomonosova[†‡§]

From the Myology Laboratory, Institute of Biomedical Problems, Russian Academy of Sciences, Moscow, Russia; the Department of Paediatrics,[†] University of Oxford, Children's Hospital, John Radcliffe, Oxford, United Kingdom; the Institute of Developmental and Regenerative Medicine,[‡] University of Oxford, Oxford, United Kingdom; and the MDUK Oxford Neuromuscular Centre,[§] Oxford, United Kingdom*

Accepted for publication February 10, 2023.

Address correspondence to Yulia Lomonosova, Ph.D., Institute of Developmental and Regenerative Medicine, University of Oxford, IMS-Tetsuya Nakamura Bldg., Old Road Campus, Roosevelt Dr., Headington, Oxford, OX3 7TY, United Kingdom.
E-mail: yulia.lomonosova@paediatrics.ox.ac.uk.

The principal mechanism underlying the reduced rate of protein synthesis in atrophied skeletal muscle is largely unknown. Eukaryotic elongation factor 2 kinase (eEF2k) impairs the ability of eukaryotic translation elongation factor 2 (eEF2) to bind to the ribosome via T56 phosphorylation. Perturbations in the eEF2k/eEF2 pathway during various stages of disuse muscle atrophy have been investigated utilizing a rat hind limb suspension (HS) model. Two distinct components of eEF2k/eEF2 pathway misregulation were demonstrated, observing a significant ($P < 0.01$) increase in eEF2k mRNA expression as early as 1-day HS and in eEF2k protein level after 3-day HS. We set out to determine whether eEF2k activation is a Ca^{2+}-dependent process with involvement of Cav1.1. The ratio of T56-phosphorylated/total eEF2 was robustly elevated after 3-day HS, which was completely reversed by 1,2-bis (2-aminophenoxy)ethane-N,N,N′,N′-tetraacetic acid—acetoxymethyl ester (BAPTA-AM) and decreased by 1.7-fold ($P < 0.05$) by nifedipine. Transfection of C2C12 with cytomegalovirus promoter (pCMV)-eEF2k and administration with small molecules were used to modulate eEF2k and eEF2 activity. More importantly, pharmacologic enhancement of eEF2 phosphorylation induced phosphorylated ribosomal protein S6 kinase (T389) up-regulation and restoration of global protein synthesis in the HS rats. Taken together, the eEF2k/eEF2 pathway was up-regulated during disuse muscle atrophy involving calcium-dependent activation of eEF2k partly via Cav1.1. The study provides evidence, *in vitro* and *in vivo*, of the eEF2k/eEF2 pathway impact on ribosomal protein S6 kinase activity as well as protein expression of key atrophy biomarkers, muscle atrophy F-box/atrogin-1 and muscle RING finger-1. *(Am J Pathol 2023, 193: 813–828; https://doi.org/10.1016/j.ajpath.2023.02.009)*

Prolonged periods of skeletal muscle inactivity, such as those associated with space flight, traumatic injuries, intensive care unit–acquired weakness, diseases, including AIDS, cancers, and neurologic disorders, and age-related muscle weakness (sarcopenia), lead to muscle atrophy characterized by reduced myofiber size and loss of muscle mass and strength.[1] It is generally accepted that disuse muscle atrophy is associated with an imbalance between anabolism and catabolism.[2] In healthy men, the primary cause of muscle wasting is impaired protein synthesis.[3] However, despite extensive effort, the mechanisms underlying the reduced rate of protein synthesis during muscle inactivity remain incompletely understood.

Hind limb suspension (HS) is the most commonly used rodent model of mechanical unloading,[3] which induces skeletal muscle atrophy. The effects of HS in the rat soleus are

Supported by Medical Research Council Research grant MR/N024850/1 (M.J.A.W.) and the Foundation for Basic Research grant RFBR11-04-01769-a (Y.L.).
Disclosures: None declared.

Copyright © 2023 American Society for Investigative Pathology. Published by Elsevier Inc. All rights reserved.
https://doi.org/10.1016/j.ajpath.2023.02.009

of particular interest as this muscle predominantly contains slow-twitch fibers, which is consistent with the fiber composition of human soleus muscle.[4,5] Furthermore, slow-twitch muscles are most affected by atrophy following mechanical unloading compared with fast-twitch muscles.[6] In previous studies, a decrease in the rate of protein synthesis was observed as early as 3 days of HS.[7] The molecular mechanisms that underlie muscle atrophy have been the subject of much investigation.[8] Akt (protein kinase B) is a master regulator involved in development of both muscle hypertrophy and atrophy.[8] The downstream consequences of Akt activation are changes in protein synthesis through the regulation of the eukaryotic translation initiation factor 2B release from glycogen synthase kinase-3β inhibition and the activation of mammalian target of rapamycin.[9] The latter, in turn, is an upstream regulator of ribosomal protein S6 kinase (p70S6k) and eukaryotic translation initiation factor 4E-binding protein 1, phosphorylation of which is necessary for translation initiation.[10] Notably, it has been shown that the phosphorylation of both p70S6k and eukaryotic translation initiation factor 4E-binding protein 1 was not impaired until 14 days of HS.[7,11,12] These observations indicate that reduced protein synthesis following initiation of HS is independent of the Akt/mammalian target of rapamycin/p70S6k cascade.

Therefore, the current study investigated alternative molecular mechanisms that may underlie disuse muscle atrophy. There is a paucity of studies on the regulation of translation elongation during muscle atrophy, although interest in the regulation of eukaryotic translation elongation factor 2 (eEF2) activity in skeletal muscle has grown in recent years.[13–15] eEF2 catalyzes the movement of peptidyl-tRNAs from the A-site to the P-site of the ribosome.[16] eEF2 is inhibited by phosphorylation at T56 conserved and specific kinase eukaryotic elongation factor 2 kinase (eEF2k).[16,17] eEF2k activity is predominantly dependent on Ca^{2+}/calmodulin.[18] However, at low intracellular calcium concentrations ($[Ca^{2+}]_i$), two additional kinases, cAMP-dependent protein kinase and AMP-activated protein kinase, can also stimulate eEF2k activity via phosphorylation at S500 and S398, respectively.[16,19] Conversely, eEF2k activity is itself inhibited by phosphorylation at S366 mediated by p70S6k and the 90-kDa ribosomal protein S6 kinase α-1.[20]

This study sought to investigate whether the eEF2k/eEF2 pathway is altered during disuse muscle atrophy. eEF2k/eEF2 cascade activity perturbations were analyzed during the various stages of atrophy development. 1,2-Bis (2-aminophenoxy)ethane-N,N,N′,N′-tetraacetic acid–acetoxymethyl ester (BAPTA-AM) and nifedipine *in vivo* were used to test whether a 4.5-fold increase in resting cytosolic free calcium concentration ($[Ca^{2+}]_i$) observed after 3 days of HS[21] promotes activation of eEF2k and whether the leakage of Cav1.1 channels (which are primarily expressed in skeletal muscle[22]) contributes to this stimulation. To determine the impact of eEF2k/eEF2 pathway perturbations on global protein synthesis on disuse, eEF2 activity was modified with two small molecules (A484954 and NH125) and eEF2k was overexpressed in C2C12 myoblasts.

Muscle atrophy F-box (MAFbx)/atrogin-1 and muscle RING finger-1 (MuRF-1) are recognized as well-known atrophy-associated biomarkers increased during muscle disuse.[23,24] There have been few studies investigating the impact of changes in activity of the factors regulating protein synthesis on MAFbx/atrogin-1 and MuRF-1 translation during muscle atrophy.[25] This area is relatively understudied in the context of muscle wasting. We hypothesize that changes in the rate of translation elongation mediated by eEF2 impact on MAFbx and MuRF-1 protein expression.

Many pathologic conditions characterized by muscle atrophy are associated with increase in glucocorticoid levels, suggesting that these hormones could trigger the muscle atrophy observed in these situations.[26] The current study tested whether activity of the eEF2k/eEF2 pathway changed in muscle atrophy induced by glucocorticoids utilizing C2C12 myotubes treated with dexamethasone (Dex).[8]

Overall, the eEF2k/eEF2 pathway was up-regulated during disuse muscle atrophy, which impacted protein synthesis initiation by modulating p70S6k activity through the regulation of MAFbx/atrogin-1 translation and an increase in eEF2k protein level. Furthermore, these data advance the understanding of cross talk of the interplay of factors involved in translation initiation and elongation.

Materials and Methods

Ethical Approval of Animal Studies

All procedures with animals were approved by the Biomedicine Ethics Committee of the Institute of Biomedical Problems of the Russian Academy of Sciences/Physiology Section of the Russian Bioethics Committee (protocol number 447; March 28, 2017). Animals were housed in a temperature-controlled room on a 12:12-hour light-dark cycle with food pellets and water provided *ad libitum*. The 3-month–old male Wistar rats ($n = 8$ per group) were obtained from the certified nursery for laboratory animals of the Institute of Bioorganic Chemistry of the Russian Academy of Sciences (Pushchino, Russia). Before all surgical procedures, the animals were anesthetized with an i.p. injection of tribromoethanol (240 mg/kg). The depth of anesthesia was evaluated by testing the pedal withdrawal reflex.

Hind Limb Suspension Model to Induce Muscle Atrophy

A widely accepted Morey-Holton hind limb suspension (HS) rodent model was utilized to induce atrophy in rats.[27] Wistar rats were randomly assigned to control (Ctrl) or HS groups. HS rats were suspended for 1, 3, 7, and 14 days. Briefly, a strip of adhesive tape was applied to the animal's tail, which was suspended by passing the tape through a swivel that was attached to a metal bar on the top of the cage. This allowed the forelimbs to have contact with the grid floor and the animals to move around. The suspension

height was adjusted to prevent the hind limbs from touching any supporting surface while maintaining a suspension angle of approximately 30 degrees.

Administration and Doses of Chemicals

Wistar rats subjected to 3 days of HS were treated with either an intracellular calcium chelator, BAPTA-AM, or a Cav1.1 blocker, nifedipine (Sigma-Aldrich, St. Louis, MO) throughout the HS period. For BAPTA-AM, each hind limb muscle was injected daily via the i.m. route with 80 μg/kg BAPTA-AM dissolved in 0.9% saline. For nifedipine, rats were injected twice per day via the i.p. route with 5 μg/kg nifedipine in 0.9% saline, as described previously.[28,29] For controls, one hind limb of each age- and sex-matched intact and HS rat was injected intramuscularly with 0.5% dimethyl sulfoxide (DMSO) in 0.9% saline for comparison with HS rats administrated with BAPTA-AM, and a contralateral hind limb was left intact for analysis of effects from nifedipine. In an independent study, each hind limb of HS rats was injected daily via i.m. route with either 38 μg/kg A484954 or 51 μg/kg NH125 (both from Tocris Bioscience, Bristol, UK) dissolved in 0.9% saline. Age- and sex-matched control and HS rats received identical vehicle exposure and were used for the comparisons. Stock solutions of BAPTA-AM, A484954, and NH125 were prepared in DMSO, and the final DMSO concentration in the saline did not exceed 0.5%.

Muscle Preparation and Weight Measurement

Under anesthesia, soleus muscles from control and suspended rats were surgically excised from both hind limbs, blotted on filter paper, tendon tissue was removed, and the muscle was weighed. To determine dry weight of soleus muscle, a half was taken, weighed, and dried at 60°C for 48 hours. The remaining tissue was flash frozen in liquid nitrogen and stored at −80°C until required for further analysis. Muscle weights were normalized to body weights and presented as a percentage of the vehicle-administered control group.

Cell Culture and Treatment

C2C12 myoblasts (ATCC, Manassas, VA) were seeded and maintained in growth medium (Dulbecco's modified Eagle's medium high glucose supplemented with 15% fetal bovine serum and 1% penicillin-streptomycin) at 37°C with 5% CO_2 for 48 hours. eEF2K expression plasmid, pCMV-eEF2K, was generated by cloning PCR-amplified eEF2k coding sequence into a mammalian expression vector driven by the human cytomegalovirus (CMV) promoter (pCMV-HA; Addgene, Watertown, MA; plasmid catalog number 32530; a gift from Christopher A. Walship, Boston Children's Hospital, Boston, MA). Oligonucleotide primers used for eEF2k coding sequence amplification are as follows: forward, 5'-ATTATTCCGCGGACCATGGCAGACGAAGA-CCTCATCTTC-3'; and reverse, 5'-ATTATTCCGCGGTTATTCCTCCATCTGGGCC-3'. The resulting plasmid construct was sequence verified. C2C12 myoblasts were transfected in 6-well format with the pCMV-eEF2k plasmid using Lipofectamine 3000 transfection reagent (catalog number L3000001; Thermo Fisher Scientific, Waltham, MA) following manufacturer's instructions. For A484954 treatment, a 1 mmol/L stock of A484954 (catalog number 4483; Tocris Bioscience) was prepared in DMSO. At 12 hours after transfection, cells were treated with A484954 diluted in growth medium to a final concentration of 1 μmol/L for 6 hours. For vehicle control, cells were mixed with the same amount of Lipofectamine 3000 and Opti-MEM (Thermo Fisher Scientific) followed by treatment with 0.1% DMSO in growth medium.

Cell viability was determined by MTS [3-(4,5-dimethylthiazol-2-yl)-5-(3-carboxymethoxyphenyl)-2-(4-sulfophenyl)-2H-tetrazolium] assay using the CellTiter 96 AQueous One Solution Cell Proliferation Assay kit (Promega, Madison, WI), according to manufacturer's protocol. Briefly, C2C12 myoblasts were plated in a 96-well plate (4000 cells per well). To estimate cytotoxicity of A484954 and pCMV-eEF2k, the cells were treated with either the inhibitor for 6 hours (concentration range, 1 nmol/L to 10 μmol/L) or the plasmid for 12 hours. The cumulative impact of both transfection and A484954 treatment was also assessed. A total of 20 μL of CellTiter AQueous Reagent was added into each well of the 96-well assay plate containing samples in 100 μL of growth medium, cells were incubated for 90 minutes in the cell culture incubator, and the absorbance was measured at 490 nm. To induce differentiation, subconfluent cell cultures were switched to differentiation medium (Dulbecco's modified Eagle's medium containing 2% horse serum and 1% penicillin-streptomycin). The first day of incubation in differentiation medium was defined as day 0 of differentiation. Differentiation medium was changed every 2 days. Dexamethasone-induced atrophy was achieved by treating cells on the fourth day of differentiation with 100 μmol/L Dex (Sigma-Aldrich) dissolved in ethanol for 48 hours, and control cells were incubated with 0.03% (v/v) ethanol (Ctrl). The treatment was repeated every 24 hours.

SUnSET Method

The surface sensing of translation (SUnSET) technique involves treatment with puromycin, an antibiotic that is a structural analogue of tyrosyl-tRNA, which can be incorporated into nascent peptide chains.[30] Subsequently, anti-puromycin antibodies are utilized to detect puromycin-incorporating peptides in protein lysates by Western blot analysis. A detailed protocol for use of the SUnSET method in rats has been described previously.[7] Briefly, rats were given an i.p. injection of 40 nmol/g puromycin hydrochloride (Enzo Life Sciences, Farmingdale, NY) dissolved in phosphate-buffered saline. At 30 minutes after injection, muscle tissue was extracted and flash frozen in liquid nitrogen for the following protein extraction. For assessment of protein synthesis in cell culture, C2C12 cells were incubated for 30 minutes with 1 μmol/L puromycin hydrochloride dissolved in

conditioned medium followed by lysis with radioimmunoprecipitation assay buffer, as described below.

RNA Isolation and quantitative RT-PCR

Total RNA was extracted using RNeasy MicroKit (Qiagen, Hilden, Germany), according to the manufacturer's recommendations. A total of 0.5 μg of RNA was reverse transcribed using the High-Capacity cDNA Reverse Transcription Kit (Thermo Fisher Scientific), according to the manufacturer's instructions. Samples to be compared were run under the same conditions (template amounts and PCR cycle duration). Details of primers designed are provided in Table 1.

Reference genes were determined using the geNorm method, and genes *Gapdh* (glyceraldehyde-3-phosphate dehydrogenase), *Ywhaz* (tyrosine 3-monooxygenase/tryptophan 5-monooxygenase activation protein ζ), and *Ppia* (peptidyl-prolyl *cis-trans* isomerase A) were selected for the purposes of normalization. The amplification was monitored using SYBR Green I and the iQ5 Multicolor Real-Time PCR Detection System (Bio-Rad Laboratories, Hercules, CA). Gene-of-interest expression was normalized to the geometric mean of stably expressed *Gapdh* and *Ppia* in rat soleus muscle, and of *Gapdh* and *Ywhaz* in C2C12. PCR efficiencies were determined empirically by amplification curve analysis using LinRegPCR and expression ratios calculated using the Pfaffl method.[31]

Protein Extraction and Western Blot Analysis

Cytoplasmic protein fractions from skeletal muscle tissue were separated and isolated using NE-PER Nuclear and Cytoplasmic Extraction kit (Thermo Fisher Scientific), following the manufacturer's instructions. Briefly, 20 mg of soleus muscle sample was homogenized and lysed in ice-cold cytoplasmic extraction reagent (CER) buffers containing phenylmethylsulfonyl fluoride (1 mmol/L; Sigma-Aldrich), protease inhibitor, and phosphatase inhibitor cocktails (both from Santa Cruz Biotechnology, Dallas, TX). C2C12 cells were washed with phosphate-buffered saline and then lysed for 20 minutes at 4°C in radioimmunoprecipitation assay buffer (Thermo Fisher Scientific) supplemented with protease inhibitor and phosphatase inhibitor cocktails (both from Sigma-Aldrich). Insoluble material was removed by centrifugation at 12,000 × *g* for 15 minutes, and supernatants were transferred to fresh tubes. Total protein concentrations were determined using the BCA Protein Assay (Thermo Fisher Scientific). Either cells or muscle lysates (15 μg) were heated at 95°C for 5 minutes in sample buffer [Laemmli Sample Buffer supplemented with 5% 2-mercaptoethanol (both from

Table 1 Nucleotide Sequences of the Primers Used for quantitative RT-PCR Analysis

Target	Gene description	Primer	RefSeq accession no.
Rat genes			
eEF2	*Eef2*	F: 5'-GTCCCCAAACAAGCACAACAGG-3' R: 5'-GGCTTCAGCAACATCCCACTCA-3'	NM_012947
eEF2k	*Eef2k*	F: 5'-AGAAGCTGGTGACAGGCAGT-3' R: 5'-GGGTTCTTGTCCAGTCCAAA-3'	NM_012947
MuRF-1	*Trim63*	F: 5'-GCCAATTTGGTGCTTTTTGT-3' R: 5'-AAATTCAGTCCTCTCCCCGT-3'	NM_080903
MAFbx	*Fbxo32*	F: 5'-CTACGATGTTGCAGCCAAGA-3' R: 5'-GGCAGTCGAGAAGTCCAGTC-3'	NM_133521
Cyclophilin A	*Ppia*	F: 5'-AGCACTGGGGAGAAAGGATT-3' R: 5'-AGCCACTCAGTCTTGGCAGT-3'	NM_017101
GAPDH	*Gapdh*	F: 5'-ACGGCAAGTTCAACGGCACAGTCAA-3' R: 5'-GCTTTCCAGAGGGGCCATCCACA-3'	NM_017008
Mouse genes			
eEF2	*Eef2*	F: 5'-GTGGTGGACTGTGTGTCTGG-3' R: 5'-CGCTGGAAGGTCTGGTAGAG-3'	NM_007907.2
eEF2k	*Eef2k*	F: 5'-CACAGAACATGCTACTCGGC-3' R: 5'-AAAGTACACGCTCCTGTCCA-3'	NM_007908.4
MuRF-1	*Trim63*	F: 5'-CTGCAGAGTGACCAAGGAGA-3' R: 5'-TTTTCCAGCTGCTCCCTG-3'	NM_001039048.2
MAFbx	*Fboxo32*	F: 5'-ACTGTCTGTTCTGTAGGCCC-3' R: 5'-CCCCACCCCAGGAATTAACT-3'	NM_026346.3
GAPDH	*Gapdh*	Mouse geNorm kit Primer Design (Chandler's Ford, UK)	NM_008084.3
14-3-3 Protein ζ/δ	*Ywhaz*	Mouse geNorm kit	NM_001253805.1

RefSeq accession numbers are available (*https://www.ncbi.nlm.nih.gov/refseq*).

F, forward; GAPDH, glyceraldehyde-3-phosphate dehydrogenase; MAFbx, muscle atrophy F-box; MuRF-1, muscle RING finger-1; R, reverse; RefSeq, reference sequence.

Table 2 List of Antibodies Used in this Study

Antibody	Dilution	Product code	Company
Puromycin	1:5000	EQ0001	Kerafast (Boston, MA)
P-eEF2 (Thr56)	1:5000	2331	Cell Signaling (Leiden, the Netherlands)
eEF2	1:5000	2332	Cell Signaling
P-eEF2k (Ser366)	1:5000	3691	Cell Signaling
eEF2k	1:5000	3692	Cell Signaling
P-p70S6k (Thr389)	1:500	9205	Cell Signaling
p70S6k	1:500	9202	Cell Signaling
P-rpS6 (Ser235/236)	1:1000	2211	Cell Signaling
P-rpS6 (Ser240/244)	1:1000	2215	Cell Signaling
rpS6	1:1000	2217	Cell Signaling
P-eIF4B (Ser422)	1:1000	3591	Cell Signaling
eIF4B	1:1000	3592	Cell Signaling
p90RSK (Thr359/Ser363)	1:1000	9344	Cell Signaling
RSK1/2/3	1:1000	9347	Cell Signaling
GAPDH	1:5000	2118	Cell Signaling
MuRF-1	1:1000	ab183094	Abcam (Cambridge, UK)
MAFbx/atrogin-1	1:1000	ab168372	Abcam
Desmin	1:1000	sc-23879	Santa Cruz Biotechnology
Anti-rabbit IgG, HRP	1:1000	7074	Cell Signaling
Anti-mouse IgG, HRP	1:1000	7076	Cell Signaling

eIF4B, eukaryotic translation initiation factor 4B; GAPDH, glyceraldehyde-3-phosphate dehydrogenase; HRP, horseradish peroxidase; MAFbx, muscle atrophy F-box; MuRF-1, muscle RING finger-1; P, phosphorylated; p70S6k, ribosomal protein S6 kinase; p90RSK, 90-kDa ribosomal protein S6 kinase; rsS6, ribosomal protein S6.

Bio-Rad Laboratories)] and subjected to PAGE and electrotransfer to polyvinylidene difluoride membrane (Thermo Fisher Scientific). To verify equal loading of protein in all lanes, the membrane was dyed with FastGreen (Bio-Rad Laboratories). The membranes were blocked for 1 hour at room temperature with Odyssey Blocking Buffer (LI-COR, Cambridge, UK) and incubated overnight at 4°C with primary antibodies diluted in Tris-buffered saline and 0.1% Tween 20 (pH 7.4). Antibodies and their dilutions are detailed in Table 2.

The membranes were washed three times for 10 minutes with Tris-buffered saline and 0.1% Tween 20 (pH 7.4) and incubated for 1 hour with horseradish peroxidase—conjugated secondary antibodies to rabbit or mouse Igs as appropriate. Following the Tris-buffered saline and 0.1% Tween 20 (pH 7.4) wash, the ImmunStar Substrate Kit (Bio-Rad Laboratories) was used to generate chemiluminescence signal. The protein bands were quantified using C-DiGit Blot Scanner and Image Studio DiGit software version 5.2.5 (LI-COR). Western blot analyses for each analyzed protein were performed at least three times. Protein-of-interest expression was normalized to GAPDH. To quantify content of puromycin-labeled proteins, Fast Green staining of total protein was used for the intensity normalization.

Immunofluorescence Staining

C2C12 myotubes were immunostained for myosin heavy chains. Myotubes were washed with phosphate-buffered saline, fixed with 4% paraformaldehyde (Santa Cruz Biotechnology), and permeabilized with 0.25% Triton X-100 (Sigma-Aldrich). Cells were then blocked with 5% bovine serum albumin (Sigma-Aldrich) before sequential incubation with primary antibodies against myosin heavy chains (MF-20; 1:100; Developmental Studies Hybridoma Bank, Iowa City, IA) and AlexaFluor 488—coupled goat—anti-mouse secondary (1:500; Thermo Fisher Scientific) antibodies. After washing with phosphate-buffered saline, cells were analyzed under a fluorescent microscope (DMI6000; Leica, Wetzlar, Germany) equipped with DFC450 acquisition camera. Subsequent image handling was performed in ImageJ software version 1.51w (NIH, Bethesda, MD; *https://imagej.net/ij/index.html*, last accessed March 13, 2018), and minimum Ferret diameter was measured with CellProfiler software version 4.2.1 (*https://cellprofiler.org*) using custom modules.

Statistical Analysis

Statistical analysis of mRNA expression and blot densitometry was performed on three technical replicates. In animal studies, data are expressed as median and interquartile range (0.25 to 0.75), with whiskers (minimum and maximum). REST 2009 version 2.0.12 software (Qiagen) was used for statistical analysis of gene expression. Statistical differences were assessed by nonparametric Newman-Keuls test utilizing GraphPad Prism 8 (GraphPad Software, La Jolla, CA). Comparisons between Ctrl and Dex-treated myotubes were tested using an unpaired *t*-test. When the means of multiple groups in C2C12 studies were compared, two-way analysis

Table 3 Time Course for Changes in Body and Muscle Weight during 1dHS, 3dHS, 7dHS, and 14dHS

Parameter	Ctrl	1dHS	3dHS	7dHS	14dHS
Rat body weight, g	240 (230–247)	230 (221–235)	229 (223–240)	235 (224–239)	230 (225–240)
Dried soleus muscle weight, mg	25.0 (23.5–27.0)	25.1 (24.4–26.8)	23.5 (22.6–25.2)	17.1 (15.8–17.7)*	15.3 (14.5–16.8)*
Dried soleus muscle weight/body weight, mg/g	0.1041 (0.1012–0.1093)	0.1093 (0.1083–1.1141)	0.1026 (0.1008–0.1053)	0.0729 (0.0676–0.0771)*	0.0671 (0.058–0077)*

Data are represented as median [interquartile range (0.25 to 0.75)].

*$P < 0.05$, significantly different from Ctrl.

1dHS, 1 day of hind limb suspension; 3dHS, 3 days of hind limb suspension; 7dHS, 7 days of hind limb suspension; 14dHS, 14 days of hind limb suspension; Ctrl, control.

of variance, followed by the Tukey *post hoc* test, was used. Differences were considered significant at the $P < 0.05$ level.

Results

Dynamic Changes in Activity of the eEF2k/eEF2 Pathway during Hind Limb Suspension–Induced Skeletal Muscle Atrophy

To investigate the various stages of atrophy development, Wistar rats were subjected to HS for 1, 3, 7, and 14 days, which covered both initial and prolonged periods of skeletal muscle inactivity ($n = 8$ per group). Untreated rats that did not undergo HS served as controls (Ctrls; $n = 8$). An approximately 40% reduction in both soleus muscle dry weight and the muscle dry weight/body weight ratio was observed at 7-day HS (Table 3), thereby confirming experimental induction of atrophy.

To investigate whether the eEF2k/eEF2 pathway was altered during the development of disuse atrophy, the expression of eEF2k and eEF2 was analyzed at both mRNA and protein levels. eEF2k mRNA levels progressively increased in the days following the HS onset, reaching a maximum of 3.5-fold at 14 days (Figure 1A). eEF2k protein expression was similarly induced in response to HS (Figure 1, B and C). In contrast, eEF2 transcript levels were unchanged in all HS groups relative to the Ctrl group (Figure 1A). The pattern of eEF2 total and phosphorylated protein levels was dynamic throughout the time course of the experiment. Significant elevation of both phosphorylated (P)-eEF2 (T56) and total eEF2 protein expression was observed as early as 1 day of HS ($P < 0.05$), resulting in an unchanged ratio of phosphorylated/total eEF2. Furthermore, robust P-eEF2 accumulation was observed after 3-day HS, reaching a peak up-regulation of the phosphorylation relative to the Ctrl rats (Figure 1, D and E). By day 7 of HS, P-eEF2 levels significantly ($P < 0.05$) reduced to that of the Ctrl rats, before increasing again at 14-day HS. eEF2 protein expression gradually declined after 1-day HS, reaching a twofold reduction by 14-day HS compared with the Ctrl (Figure 1D). Nevertheless, the ratio of phosphorylated/total eEF2 protein at 7- and 14-day HS remained elevated and did not differ from that in the 3-day HS group (Figure 1E).

It has previously been shown in embryonic stem cells that both p70S6k and 90-kDa ribosomal protein S6 kinase α-1 phosphorylate eEF2k at a single serine residue (S366), leading to its inactivation.[20] A twofold decrease in eEF2k S366 phosphorylation was observed after 1 day of HS, consistent with eEF2k activation in response at this time point (Figure 1F). In contrast, from 3-day HS until 14-day HS, P-eEF2k (S366) level was twofold elevated, concomitant with an equivalent increase in total eEF2k content, resulting in an unchanged ratio of P-eEF2k(S366)/eEF2k (Figure 1, C and F).

The data show that the eEF2k/eEF2 signaling pathway is dynamically regulated in response to disuse-associated muscle atrophy, with the onset of pathway perturbations occurring early (ie, at 3 days) during the HS period. Notably, the ratio of phosphorylated/total eEF2 protein was still elevated after 3 days of HS, although up-regulation of eEF2k inhibitory phosphorylation at S366, mediated by p70S6k, was observed. This suggests that there is an additional factor contributing to eEF2k activation during HS.

eEF2k Activation during Hind Limb Suspension Is Calcium Dependent

It was hypothesized that the elevation in intracellular Ca^{2+} observed as early as 2 days of HS[21,32] results in up-regulation of eEF2k activity, thereby leading to an increase in eEF2 phosphorylation. The study set out to determine whether the leakage of Cav1.1 channels (which are primarily expressed in skeletal muscle[22]) contributes to the $[Ca^{2+}]_i$ elevation and eEF2k stimulation during disuse. To test this hypothesis, Wistar rats were subjected to 3-day HS and treated with either a calcium chelator, BAPTA-AM, or an inhibitor of Cav1.1 channels, nifedipine ($n = 8$ per group). To confirm that treatment with BAPTA-AM and nifedipine reduced the $[Ca^{2+}]_i$ elevation, the content of the cytoskeletal protein desmin was evaluated. Desmin

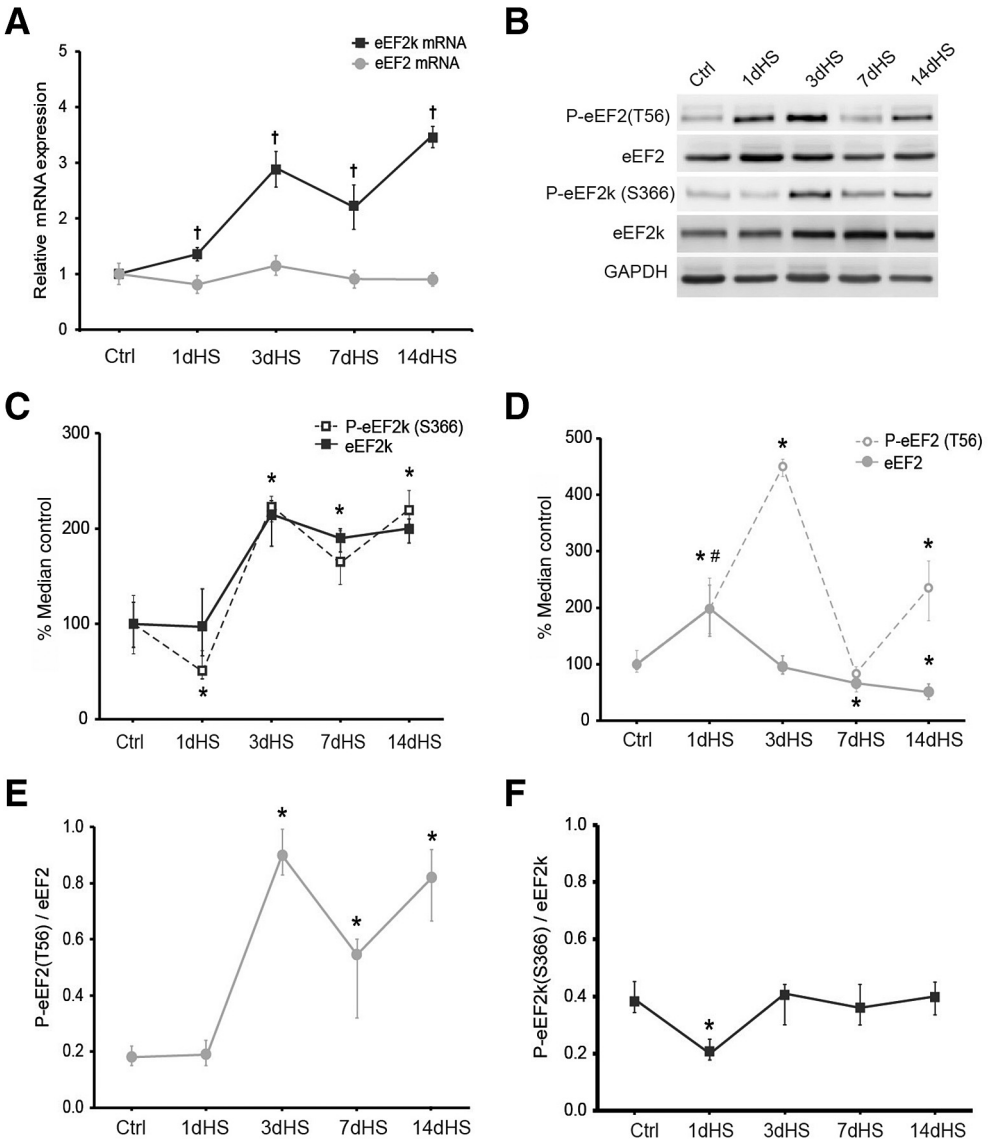

Figure 1 Differential expression of the eEF2k/eEF2 signaling pathway in muscle in response to hind limb suspension (HS). The 3-month—old male Wistar rats were randomly assigned to untreated control (Ctrl) and HS groups. HS was performed for 1, 3, 7, and 14 days (1dHS, 3dHS, 7dHS, and 14dHS, respectively). **A:** Relative mRNA levels of eEF2k and eEF2 were determined by quantitative RT-PCR. **B:** Representative images of Western blot analyses of phosphorylated (P)-eEF2 (T56), eEF2, P-eEF2k (S366), and eEF2k. Fast Green staining for total protein and glyceraldehyde-3-phosphate dehydrogenase (GAPDH) were used for loading control and normalization of band intensity for proteins of interest. **C—F:** Western blot densitometric analysis of eEF2 and eEF2k levels and P-eEF2 (T56)/eEF2 and P-eEF2k (S366)/eEF2k ratios. mRNA and total protein levels in the HS groups are expressed as fold or percentage changes relative to the Ctrl. Quantification of phosphorylation level of protein of interest was calculated using the ratio of phosphorylated protein band intensity/band intensity of the total form on Western blot analysis. Data are represented as median, and whiskers show interquartile range (0.25 to 0.75; **A** and **C—F**). $n = 8$ rats per group. $^{*}P < 0.05$, $^{\dagger}P < 0.01$, significant difference from the Ctrl group; $^{\#}P < 0.05$, significant difference of total eEF2 in the 1dHS group from the Ctrl (Newman-Keuls test).

expression is commonly used as an indicator of $[Ca^{2+}]_i$ as its degradation is mediated by Ca^{2+}-dependent protease μ-calpain.[33] Proteolysis of desmin was confirmed in the HS rats, and both BAPTA-AM and nifedipine fully prevented its degradation (Figure 2, A and B). Notably, the activity of μ-calpain is sensitive to Cav1.1 activation.[21] Treatment of HS rats with BAPTA-AM and nifedipine had no effect on mRNA and protein expression levels for either eEF2 or eEF2k (Figure 2, C and D). As in the time-course experiment described above (Figure 1, C—E), phosphorylation at the eEF2 T56 site was increased in the HS group, and this increase was completely reversed by BAPTA-AM (Figure 2E). Similarly, nifedipine resulted in a partial reversal of eEF2 phosphorylation. P-eEF2 (T56) levels were reduced by approximately twofold relative to HS alone, although they remained significantly ($P < 0.05$) elevated relative to the Ctrl group (Figure 2E). BAPTA-AM reduced phosphorylation of eEF2k at S366 site (Figure 2F). SUnSET

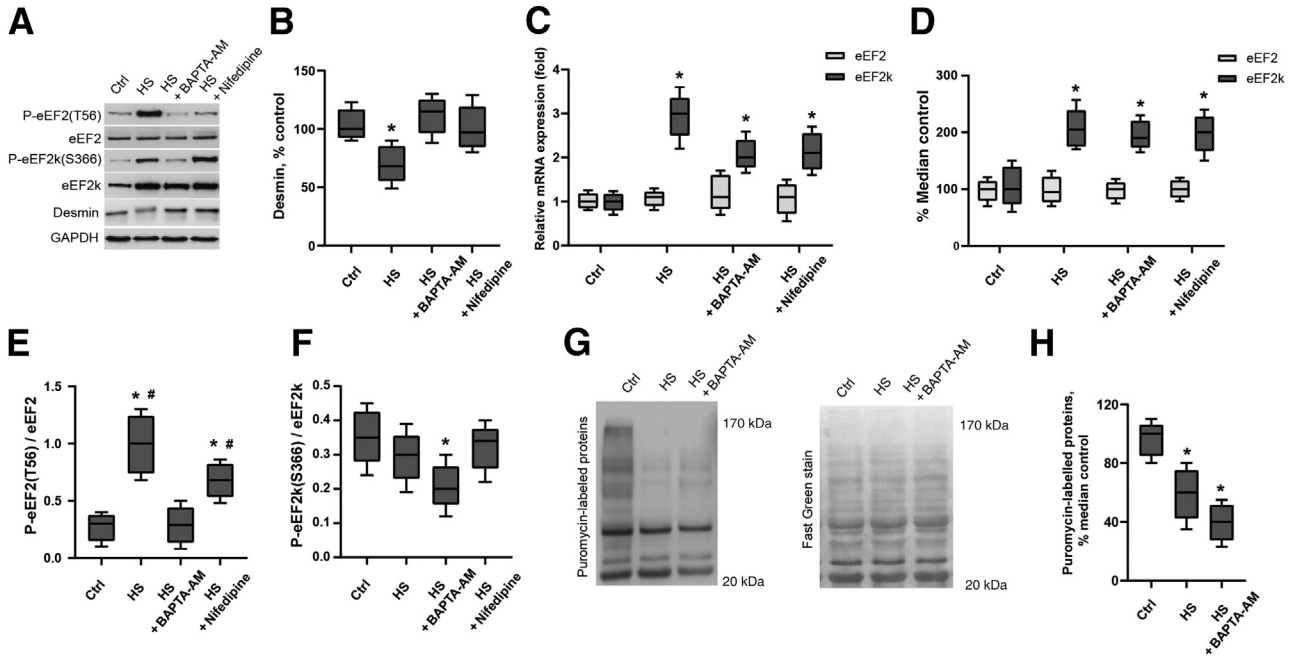

Figure 2 Calcium-dependent regulation of the eEF2k/eEF2 signaling pathway on hind limb suspension (HS). Wistar rats were suspended for 3 days (HS), and some HS rats were randomly selected for either BAPTA-AM (HS + BAPTA-AM) or nifedipine (HS + nifedipine) daily treatment. **A:** Representative images of Western blot analyses of phosphorylated (P)-eEF2 (T56), eEF2, P-eEF2k (S366), eEF2k, desmin, and glyceraldehyde-3-phosphate dehydrogenase (GAPDH). **B:** Desmin content as a marker of BAPTA-AM and nifedipine treatment to reduce the $[Ca^{2+}]_i$ elevation. **C:** Relative mRNA levels of eEF2k and eEF2 were determined by quantitative RT-PCR. **D:** Values of eEF2 and eEF2k proteins in the HS groups are expressed as percentage changes in comparison with the control (Ctrl) values. **E** and **F:** The ratio of phosphorylated protein form band intensity/band intensity of total form of the protein was used for estimation of phosphorylation level of eEF2 and eEF2k at T56 and S366 sites, respectively. **G:** SUnSET method was utilized for measurement of protein synthesis in the Ctrl, HS, and HS + BAPTA-AM groups. To quantify content of puromycin-labeled proteins, Fast Green staining of total protein was used for the intensity normalization. **H:** Values of puromycin-labeled total protein in the HS groups are expressed as percentage changes in comparison with the Ctrl values. Data are represented as median, box shows interquartile range (0.25 to 0.75), and whiskers show minimum and maximum (**B**–**F** and **H**). $n = 8$ rats per group. $^{*}P < 0.05$, significant difference from the Ctrl group; $^{\#}P < 0.05$, significant difference from the HS + BAPTA-AM group (Newman-Keuls test).

method was used to show a 40% reduction in the protein synthesis rate after 3-day HS (Figure 2, G and H). Cotreatment of HS rats with BAPTA-AM was insufficient to reverse the HS-associated reduction in protein synthesis (Figure 2H). Similarly, both BAPTA-AM and nifedipine treatments had no effect on the muscle dried weight and the muscle dried weight/body weight ratio at 3 days of HS (Supplemental Table S1).

Overall, these findings demonstrate that the up-regulation of eEF2k activity during HS is a calcium-dependent process, driven partly by Cav1.1 channels and not dependent on the S366 phosphorylation mediated by p70S6k.

Stimulation of eEF2 Hyperphosphorylation Restores the Rate of Protein Synthesis in Soleus Muscle of HS Rats

Rats subjected to 3 days of HS were treated daily throughout the HS period with two small-molecule drugs that exert opposing effects on eEF2 phosphorylation. A484954 is an inhibitor of eEF2k, which is therefore expected to diminish eEF2 inactivation by phosphorylation at T56. NH125 has been shown to induce eEF2 hyperphosphorylation.[34] Surprisingly, NH125 treatment fully prevented a decrease in the rate of protein synthesis in soleus muscle induced by HS (Figure 3, A and B). eEF2 mRNA and protein expression levels were stable in all experimental groups (Figure 3, C–E). A484954 reduced eEF2k mRNA expression compared with HS rats, although eEF2k protein levels remained elevated in the HS + A484954 group (Figure 3, C–E). NH125 had no effect on either eEF2 or eEF2k transcript and protein levels during HS (Figure 3, C–E). A484954 completely prevented the increase in P-eEF2 level at 3-day HS, thereby demonstrating effective inhibition of eEF2k activity (Figure 3F). As expected, NH125 administration during 3-day HS led to 1.5-fold up-regulation of P-eEF2 (T56) levels compared with the HS (Figure 3F). In addition, robust phosphorylation of eEF2k was observed at S366 in the HS + NH125 group (Figure 3G) mediated by p70S6k, which was threefold higher than that in the HS. A 3.5-fold increase in P-p70S6k (T389) levels was observed in the HS + NH125 rats compared with those in HS rats (Figure 3H), suggesting an increase in p70S6k activity.

A484954 had no effect on phosphorylation level of eEF2k at S366 residue in the HS rats (Figure 3G). Similarly, no changes in the p70S6k phosphorylation were observed in

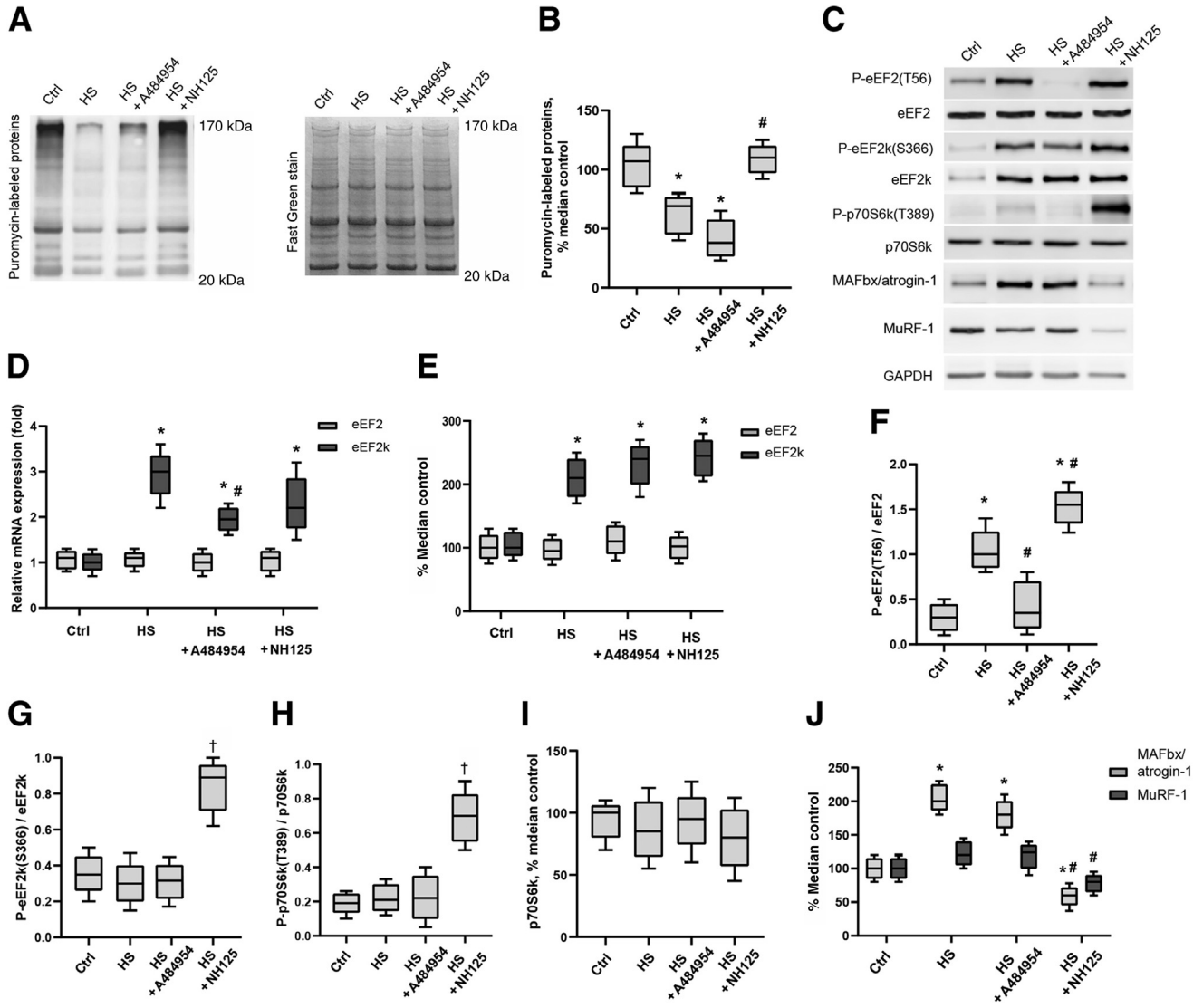

Figure 3 Involvement of the eEF2k/eEF2 pathway in protein synthesis impairment during hind limb suspension (HS). The 3-day HS rats were injected daily with saline (HS), A484954 (HS + A484954), or NH125 (HS + NH125). **A:** SUnSET method was utilized for measurement of protein synthesis. Fast Green staining was used for the intensity normalization to quantify content of puromycin-labeled proteins. **B:** Puromycin-labeled total protein contents in the HS groups are expressed as percentage changes relative to the control (Ctrl) group. **C:** Representative images of Western blot analyses of phosphorylated (P)-eEF2 (T56), eEF2, P-eEF2k (S366), eEF2k, P-ribosomal protein S6 kinase (p70S6k) (T389), p70S6k, muscle atrophy F-box (MAFbx)/atrogin-1, muscle RING finger-1 (MuRF-1), and glyceraldehyde-3-phosphate dehydrogenase (GAPDH). **D:** Relative mRNA levels of eEF2 and eEF2k were determined by quantitative RT-PCR. mRNA levels in each HS group are expressed as a fold of the Ctrl. **E**–**J:** Quantitative analysis of total eEF2, eEF2k, p70S6k, and their phosphorylation at T56, S366, and T389 sites, respectively, as well as total MAFbx/atrogin-1 and MuRF-1 levels were assessed in the HS groups relative to the Ctrl. Values of total forms of the proteins in the transfected cells are expressed as percentage changes relative to the Ctrl values set as 100%. The ratio of phosphorylated protein band intensity/band intensity of a total form of the protein was used for estimation of phosphorylation level. Data are represented as median, box shows interquartile range (0.25 to 0.75), and whiskers show minimum and maximum (**B** and **D**–**J**). $n = 8$ rats per group. $^{*}P < 0.05$, significant difference from the Ctrl group; $^{\#}P < 0.05$, significant difference from the HS group; $^{\dagger}P < 0.05$, significant differences from all other groups (Newman-Keuls test).

either HS or HS + A484954 groups (Figure 3H). Total p70S6k protein was unchanged across all groups (Figure 3I). The components of the 40S ribosomal protein S6 (rpS6) and eukaryotic translation initiation factor 4B (eIF4B) are known substrates for p70S6k.[35] Consistent with the protein synthesis decrease, a significant ($P < 0.05$) down-regulation of phosphorylation levels of rpS6 at S235/236 and S240/244 sites and the amount of P-eIF4B (S422) was observed in the HS and HS + A484954 groups compared with the Ctrl rats (Supplemental Figure S1). These findings show that, despite unchanged level of p70S6k phosphorylation, activity of its downstream substrates was reduced in the HS rats injected with A484954 or saline.

Up-regulation of both MAFbx/atrogin-1 and MuRF-1 mRNA was observed in the HS rats (Supplemental Figure S2). A twofold increase in MAFbx/atrogin-1 protein expression was observed at 3-day HS (Figure 3J). No

changes in MAFbx/atrogin-1 and MuRF-1 protein levels were seen by the third day of HS treated with A484954. Consistent with the reduced eEF2 activity via T56 hyperphosphorylation, both MuRF-1 and MAFbx/atrogin-1 protein expression were significantly ($P < 0.05$) decreased in the HS + NH125 rats compared with the HS group (Figure 3J).

In summary, the study indicates that enhanced inhibition of eEF2 promoted an increase in p70S6k phosphorylation as well as preserved the rate of total protein synthesis on HS, suppressing accumulation of E3-ubiquitin ligases MAFbx/atrogin-1 and MuRF-1. In addition, the p70S6k activation leads to an increase in S366 phosphorylation of eEF2k; however, it fails to inhibit its activity. Restoration of eEF2 function alone did not rescue global protein synthesis. More importantly, activity of p70S6k downstream substrates rpS6 and eIF4B was impaired in the HS groups both with and without A484954 treatment, consistent with the suppression of protein synthesis.

Up-Regulation of eEF2k in C2C12 Myoblasts Suppresses Initiation Factors and Decreases the Rate of Global Protein Synthesis

To investigate the impact of the eEF2k/eEF2 pathway on protein synthesis impairment, eEF2k activity was modulated in C2C12 myoblasts by overexpression of eEF2k with and without A484954. No cytotoxic effects were observed for any of the treatments (Supplemental Figure S3). A threefold increase in eEF2k protein expression was observed after plasmid transfection (Figure 4, A and B), with a corresponding twofold increase in the eEF2 phosphorylation level (Figure 4C). No significant changes in the expression of total eEF2 were observed in C2C12 overexpressing eEF2k (both with and without A484954 treatment) relative to untreated Ctrl (Figure 4D). However, a reduction in eEF2k activity was observed as the phosphorylation level of eEF2 (T56) was equal to the level observed in the Ctrl group (Figure 4C). Notably, activation of the eEF2k/eEF2 cascade down-regulated MAFbx/atrogin-1 protein expression, and A484954 reversed this effect (Figure 4E). Similar to animal studies, an increase in eEF2k protein expression in the transfected myoblasts led to up-regulation of eEF2k S366 phosphorylation mediated by p70S6k (Figure 4H).

An increase in eEF2k protein expression in the transfected myoblasts did not change total p70S6k protein expression but led to up-regulation of its T389 phosphorylation (Figure 4, F and G) accompanied by an increase in phosphorylation of eEF2k at S366 site (Figure 4H). The p70S6k phosphorylation was reduced to the level observed in the Ctrl after A484954 treatment (Figure 4G). Despite a decrease in P-p70S6k content following the eEF2k inhibition, the phosphorylation level of eEF2k at S366 remained elevated, as in the transfected cells without treatment (Figure 4H). This indicates that when up-regulated, eEF2k protein undergoes inhibitory *trans* phosphorylation at S366 site regulated by p70S6k. p70S6k T389 phosphorylation, in turn, is dependent on eEF2 activity. To estimate the protein synthesis rate after eEF2k overexpression, C2C12 cells were treated with puromycin, and the SUnSET method was performed (Figure 5A). More important, an approximately 40% reduction in the rate of mRNA translation was observed following eEF2k up-regulation, which was not rescued when transfected cultures were cotreated with A484954 (Figure 5B).

When analyzing downstream substrates of p70S6k, phosphorylation status of rpS6 at S235/236 and S240/244 and eIF4B at S422 was dramatically decreased in myoblasts overexpressing eEF2k in both the presence and the absence of A484954 (Figure 5, C–E). Notably, rpS6 and eIF4B are also substrates for 90-kDa ribosomal protein S6 kinase family.[35] Analysis of phosphorylation of 90-kDa ribosomal protein S6 kinase at T359/S363 did not reveal any changes in its activity (Figure 5F). Both the transfection and A484954 treatment did not change content of rpS6, eIF4B, or p90 ribosomal S6 kinase (RSK) total forms in C2C12 (Figure 5, G–I).

Overall, these data show that up-regulation of eEF2k resulted in inhibition of eEF2 in addition to the decreased activity of translation initiation factors, thereby resulting in a reduction in protein synthesis.

Dexamethasone Induces Down-Regulation of Total and T56-Phosphorylated Forms of eEF2

Many pathologic conditions characterized by muscle atrophy (starvation, cachexia, and sepsis) are associated with an increase in circulating glucocorticoids levels, suggesting that these hormones could trigger the muscle atrophy observed in these situations.[26,36] Whether activity of the eEF2k/eEF2 pathway was changed on skeletal muscle atrophy induced by glucocorticoids was tested with C2C12 murine myotubes treated with Dex.[8,37] Myotube atrophy was induced in differentiated C2C12 via treatment with Dex, as described previously,[23] resulting in a significant ($P < 0.05$) decrease in myotube diameter (Figure 6, A and B). As expected, Dex treatment induced an increase in expression of atrophy-associated factors E3-ubiquitin ligases, MAFbx/atrogin-1, and MuRF-1, at both mRNA and protein levels (Figure 6, C–E). eEF2k and eEF2 mRNA levels were unaffected by Dex (Figure 6F). However, Dex induced a decrease in both total and phosphorylated forms of eEF2, resulting in an overall unchanged ratio of eEF2 (Figure 6, G and H). Furthermore, Dex did not influence either eEF2k protein expression or its phosphorylation level (Figure 6I). When analyzing the activity of p70S6k in Dex-treated myotubes, a twofold decrease in both total p70S6k and its phosphorylated form was observed compared with Ctrl, which resulted in an unchanged phosphorylation ratio of p70S6k (Figure 6, J and K). There was no change in the protein synthesis rate in Dex-treated myotubes, as determined by SUnSET analysis (Figure 6, L and M).

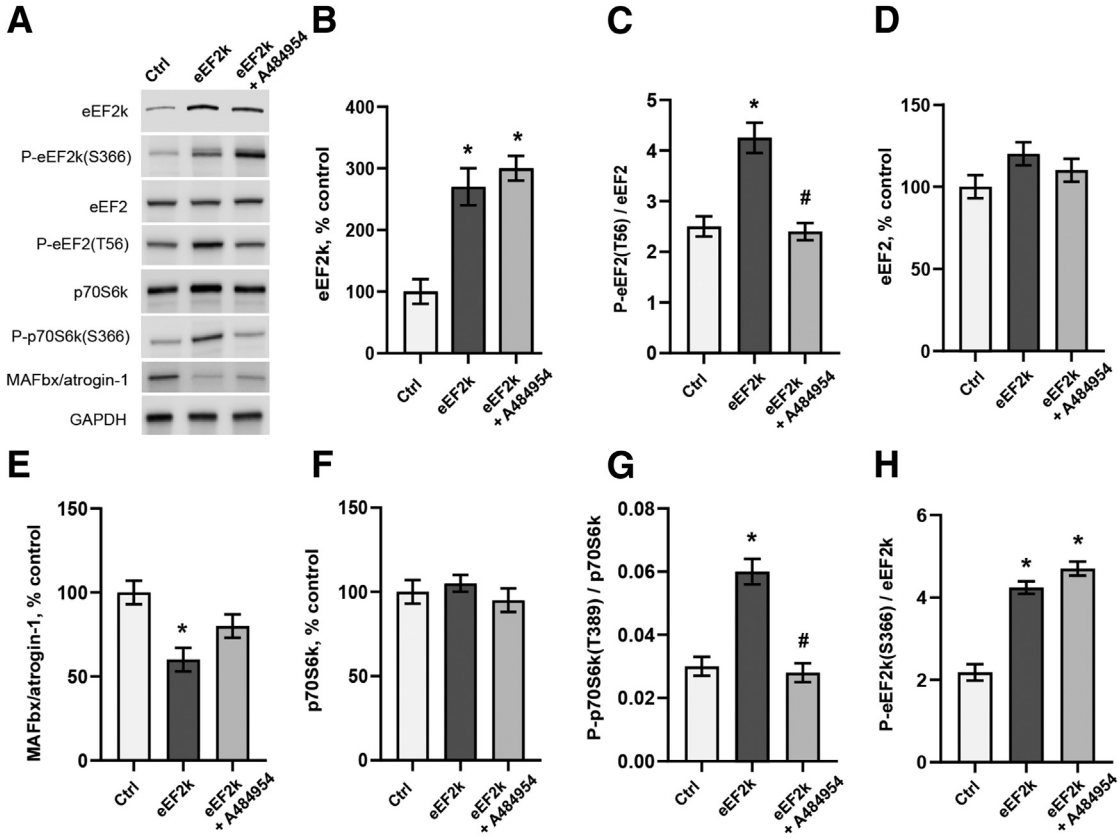

Figure 4 eEF2k up-regulation promotes eEF2 and ribosomal protein S6 kinase (p70S6k) phosphorylation as well as a reduction in muscle atrophy F-box (MAFbx)/atrogin-1 protein expression in C2C12. C2C12 myoblasts were transfected with the pCMV-eEF2k plasmid (eEF2k), together with A484954 treatment (eEF2k + A484954). Untransfected C2C12 myoblasts are indicated as control (Ctrl). **A:** Representative images of Western blot analyses of total and phosphorylated (P) forms of eEF2k, eEF2, and p70S6k as well as total MAFbx/atrogin-1. Fast Green staining for total protein and glyceraldehyde-3-phosphate dehydrogenase (GAPDH) expression were used for loading control and normalization of band intensity for proteins of interest. **B**—**D:** Quantitative analysis of pCMV-eEF2k transfection with or without A484954 treatment on eEF2k, eEF2 protein expression, and eEF2 T56 phosphorylation. **E**—**H:** Quantitative analysis of eEF2k up-regulation with or without A484954 on total MAFbx/atrogin-1, p70S6k, and phosphorylation of p70S6k and eEF2k at T389 and S366, respectively. Values of total forms of the proteins in the transfected cells are expressed as percentage changes relative to the Ctrl values set as 100%. The ratio of phosphorylated protein band intensity/band intensity of a total form of the protein was used for estimation of phosphorylation level. Data are represented as means ± SEM (**B**—**H**). $n = 3$ per group. $^{*}P < 0.05$, significant difference from the Ctrl group; $^{\#}P < 0.05$, significant difference from the eEF2k group (two-way analysis of variance with Tukey test).

These data show that Dex administration induced activation of proteolysis with involvement of E3-ubiquitin ligases, which likely resulted in a decrease in p70S6k and eEF2 protein expression, in addition to a reduction in myotube diameter.

Discussion

This study first sought to investigate whether the eEF2k/eEF2 signaling pathway is altered during disuse-induced skeletal muscle atrophy. It utilized HS in rats, the most common and well-studied model of disuse-induced skeletal muscle atrophy.[38]

Various stages in the development of muscle atrophy were investigated, from the first day of disuse until 2-week period when drastic changes in both molecular pathways and morphology of muscle can be observed.[39] Atrophy progression in muscle soleus of rats subjected to HS was confirmed, showing a reduction in muscle weight after 7 days of suspension. eEF2k impairs the ability of eEF2, the only known substrate for eEF2k, to bind to the ribosome via T56 phosphorylation, thereby slowing the elongation phase of protein synthesis.[18,40] Having investigated the eEF2/eEF2 pathway over 14 days of atrophy progression, we proposed two different stages of the cascade perturbations.

The study demonstrated an increase in eEF2k mRNA expression but not in its protein levels as early as 1 day following the HS onset. Interestingly, an increase in the amount of the phosphorylated eEF2 protein was observed. This can be a result from either the eEF2 substrate increase or relaxation of the inhibitory S366 phosphorylation of eEF2k mediated by p70S6k, with ratio of phosphorylated/total eEF2k protein decreasing. An increase in p70S6k activity has been reported previously[7]; however, a decrease in

eEF2k S366 phosphorylation at the 1-day time point of the HS onset was observed here. S366 phosphorylation reduces eEF2k activity at basal or low (physiologically relevant) $[Ca^{2+}]_i$; however, this inhibition is eliminated at high $[Ca^{2+}]_i$.[20,41] Therefore, the decrease in eEF2k S366 phosphorylation at 1-day HS can be explained by elevated $[Ca^{2+}]_i$,[21] which could compete with the effects of p70S6k-mediated inhibition. However, the increased eEF2k activity unlikely resulted in impairment of eEF2 activity in the 1-day HS rats, taking into consideration the unchanged ratio of active unphosphorylated eEF2 molecules. This supports the hypothesis that, during onset of HS, eEF2 performs its function of peptide elongation as in healthy animals. Notably, a reduction in the protein synthesis rate has not been reported at the 1-day time point following induction of HS in rats.[7]

After 3 days of HS, the earliest time point when a decrease in global protein synthesis has been reported in HS rats,[7] the second stage of evolving eEF2k/eEF2 pathway perturbation was observed, manifesting an

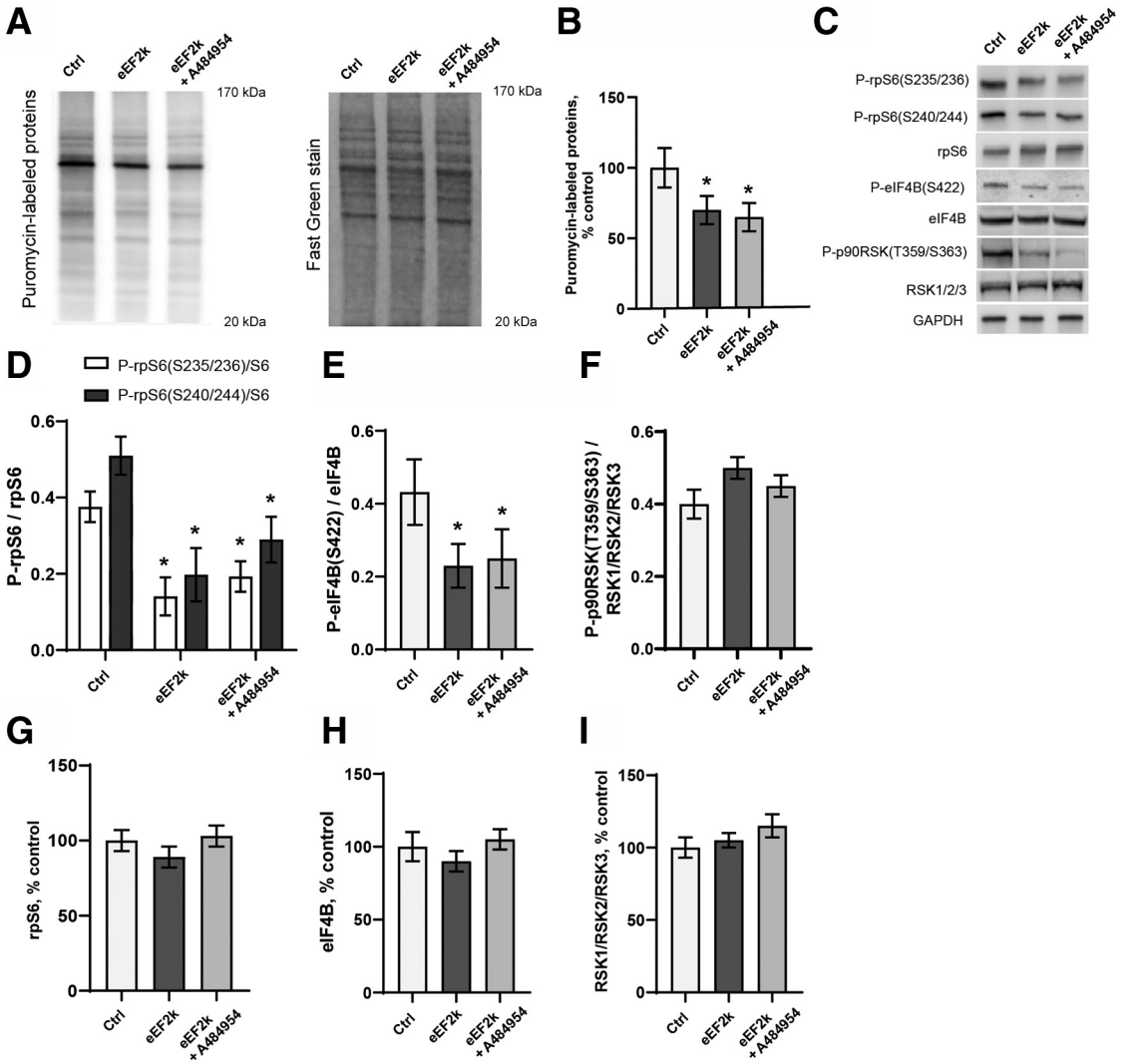

Figure 5 Effect of eEF2k up-regulation on the protein synthesis rate and translation initiation factors in C2C12. **A:** At 30 minutes before harvest, cells were incubated with 1 μmol/L puromycin to monitor the protein synthesis rate via the SUnSET method. Fast Green staining was used for the intensity normalization to quantify content of puromycin-labeled proteins. **B:** Values of puromycin-labeled total protein in the eEF2k and eEF2k + A484954 groups are expressed as percentage changes in comparison with untransfected C2C12 [control (Ctrl)] values set as 100%. **C:** Representative images of Western blot analyses showing staining of total and phosphorylated (P) forms of ribosomal protein S6 (rpS6), eukaryotic translation initiation factor 4B (eIF4B), and 90-kDa ribosomal protein S6 kinase α-1/2/3 (p90RSK1/2/3) at multiple sites after pCMV-eEF2k transfection with or without A484954 treatment. Fast Green staining for total protein and glyceraldehyde-3-phosphate dehydrogenase (GAPDH) were used for loading control and normalization of band intensity for the proteins. **D**—**F:** The ratio of phosphorylated protein band intensity/band intensity of a total form of the protein was used for estimation of phosphorylation level of rpS6 at S235/S236 and S240/S244 sites, eIF4B at S422 site, and RSK1/2/3 at T359/S363 sites. **G**—**I:** Values of rpS6, eIF4B, and RSK1/2/3 protein levels are expressed as percentage changes relative to the values of untransfected cells (Ctrl) set as 100%. Data are represented as means ± SEM (**B** and **D**—**I**). $n = 3$ per group. $^*P < 0.05$, significant difference from Ctrl group (two-way analysis of variance with Tukey test).

increase in eEF2k protein expression accompanied by the elevation of the P-eEF2(T56)/eEF2 ratio. This was consistent with the similarly elevated eEF2k protein levels at 3, 7, and 14 days of HS. In the animal studies and in the C2C12-overexpressing eEF2k, p70S6k responded to an increase in eEF2k protein expression by intensifying its S366 phosphorylation, which likely induced a decrease in activity of p70S6k downstream factors rpS6 and eIF4B contributing to translation initiation. Indeed, overexpression of eEF2k in C2C12 myoblasts, in addition to an elevation in eEF2 T56 phosphorylation, led to decreased rpS6 and eIF4B phosphorylation, thereby impairing the protein synthesis rate. More importantly, inhibition of eEF2k activity and restoration of eEF2 phosphorylation did not reverse the decrease in the protein synthesis rate, which is in good agreement with our findings in the rat HS model (Supplemental Figure S1). Accordingly, theses data suggest that eEF2k might compete with other downstream substrates of p70S6k, therefore impairing protein synthesis initiation.

eEF2 protein could perhaps undergo degradation at a later stage of disuse not covered in the current study, given that eEF2 protein level was gradually decreasing after 7-day HS at unchanged eEF2 mRNA level over the HS time points and may not be terminated at the 14-day HS. Interestingly, a dramatic decrease in the eEF2

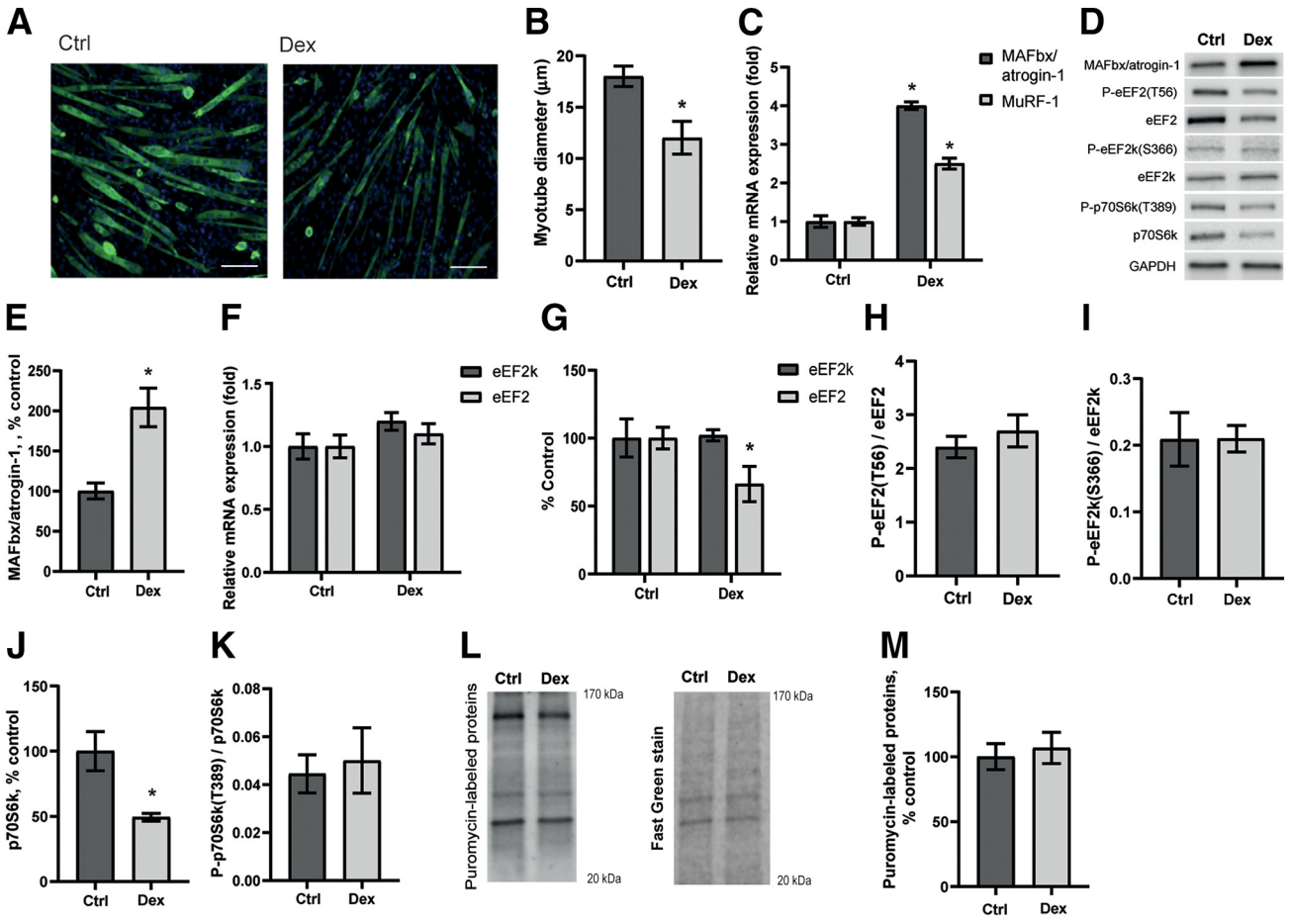

Figure 6 Effect of dexamethasone (Dex) treatment on C2C12 myotubes. **A:** Immunostaining of myotube cultures treated with vehicle [control (Ctrl)] and 100 μmol/L Dex for 48 hours. Immunofluorescence analysis was performed using myosin heavy chain antibody. **B:** The diameter of myotubes treated with Dex was estimated using CellProfiler software version 4.2.1. **C** and **F:** Expression of muscle atrophy F-box (MAFbx)/atrogin-1, muscle RING finger-1 (MuRF-1), eEF2k, and eEF2 mRNA levels was assessed by quantitative RT-PCR. Values for the Ctrl group are set at 1. **D:** Western blot analysis shows effect of Dex treatment on puromycin-labeled proteins, MAFbx/atrogin-1, total and phosphorylated (P) forms of eEF2, eEF2k, and ribosomal protein S6 kinase (p70S6k). **E**, **G**, and **J:** Changes in MAFbx/atrogin-1, eEF2k, eEF2, and p70S6k protein content and their phosphorylated forms were tested with Western blot analysis. Values of MAFbx/atrogin-1, eEF2k, eEF2, and p70S6k are expressed as percentage changes relative to the Ctrl. **H**, **I**, and **K:** The ratio of phosphorylated protein band intensity/band intensity of total form of protein was used for estimation of phosphorylation level of eEF2, eEF2k, and p70S6k at T56, S366, and T389 sites, respectively. **L:** At 30 minutes before harvest, cells were incubated with 1 μmol/L puromycin to monitor the protein synthesis rate via the SUnSET method. Fast Green staining was used for the intensity normalization to quantify content of puromycin-labeled proteins. **M:** Values of puromycin-labeled total protein are expressed as percentage changes relative to the Ctrl values. Data are represented as means ± SEM (**B**, **C**, **E**–**K**, and **M**). $n = 3$ per group. $^*P < 0.05$, significant difference from the Ctrl group (unpaired *t*-test). Scale bars = 50 μm (**A**). GAPDH, glyceraldehyde-3-phosphate dehydrogenase.

phosphorylation was observed at the 7-day HS, when the decreased eEF2 level was first detected, possibly inducing an elimination in eEF2k activity toward its substrate. However, the enhanced eEF2 phosphorylation was reversed by 14th day of HS. Taking together, these findings show alterations in the eEF2k/eEF2 pathway during development of disuse muscle atrophy are highly dynamic and complex, involving changes in transcript and protein expression as well as in phosphorylation of both eEF2 and eEF2k. This indicates that an increase in eEF2k S366 phosphorylation, mediated by p70S6k, does not suppress eEF2k activity during disuse, because the proportion of active eEF2k molecules does not exceed that in healthy animals and does not lead to eEF2k suppression, which is supported by analysis of eEF2 T56 phosphorylation.

Whether activation of Ca^{2+}/calmodulin-dependent eEF2k during HS is calcium dependent was tested, given that basal $[Ca^{2+}]_i$ reaches a 4.5-fold elevation after 3 days of HS and the leakage through Cav1.1 channels contributes to this process.[21] To this end, 3-day HS rats were treated with either a cell-permeant highly selective calcium chelator, BAPTA-AM, or a Cav1.1 inhibitor, nifedipine, using established protocols,[21,42,43] which demonstrated that eEF2k activity is calcium dependent. Notably, blockage of Cav1.1 did not rescue elevation of eEF2 phosphorylation completely, indicating that calcium available for eEF2k activation is affected not only by the leakage through Cav1.1, but also can involve other means of calcium entry (eg, via store-operated channels and ryanodine receptors).[44] Furthermore, the impairment of the calcium reuptake from the sarcoplasm to the main calcium storage in the muscle, such as the sarcoplasmic reticulum, believed to be induced by sarco/endoplasmic reticulum Ca-ATPase (SERCA) inactivation might also contribute to the eEF2k activation.[45]

In regards to eEF2k phosphorylation, it is not surprising that different effects of the compounds were observed on the phosphorylation of S366, considering their differential impact on calcium depletion.[46] The relatively smaller magnitude change in $[Ca^{2+}]_i$, mediated by nifedipine, is insufficient to modulate eEF2k phosphorylation at S366 during HS. The current data indicate that increased activity of eEF2k during disuse muscle atrophy is a calcium-dependent process driving partly by Cav1.1 and not dependent on the S366 phosphorylation modulated by p70S6k.

When applying NH125 to analyze impact of eEF2 hyperphosphorylation on global protein synthesis *in vivo* in the condition of atrophy, complete restoration of the protein synthesis rate was unexpectedly observed in HS rats. We propose that the activation of p70S6k following NH125 treatment observed in these rats is sufficient to maintain protein synthesis at the levels corresponding to those in healthy muscle. When analyzing the impact of eEF2 hyperphosphorylation on the protein expression of atrophy biomarkers MAFbx/atrogin-1 and MuRF-1, a dramatic decrease in their elevation was observed. The coordinated activity of p70S6k and eEF2 can be explained by changes in MAFbx/atrogin-1 protein expression. MAFbx/atrogin-1 degrades its major target, such as eukaryotic initiation factor 3 subunit f, which, in turn, suppresses p70S6k activation.[47] This was confirmed in the transfected C2C12 myoblasts showing enhanced eEF2 inhibition and an increase in p70S6k phosphorylation accompanied by a decrease in MAFbx/atrogin-1 protein expression. This effect was reversed by eEF2k inhibitor, which supports involvement of eukaryotic initiation factor 3 subunit f. A484954 reversed eEF2 T56 phosphorylation; however, it did not restore global protein synthesis in HS rats. Taken together, the data indicate that restoration of eEF2 function alone does not rescue global protein synthesis in skeletal muscle exposed to disuse.

Dex has an atrophic effect on C2C12 myotubes,[8] which is employed as an *in vitro* model of glucocorticoid-induced skeletal muscle atrophy. The development of atrophy was confirmed by a decrease in myotube diameter along with intensification of MAFbx/atrogin-1 and MuRF-1 expression. Similar to 7- and 14-day HS, down-regulation in eEF2 protein levels were observed in Dex-treated myotubes, which supports involvement of the ubiquitin-proteasome system in eEF2 degradation. The unchanged phosphorylation status of both p70S6k and eEF2 proteins responsible for the translation initiation and elongation, respectively, might explain absence of protein synthesis impairment on 2-day Dex treatment. Previously published data on the investigation of protein synthesis are controversial. When analyzing anabolic changes in myotubes after Dex treatment, most studies have primarily evaluated only Akt phosphorylation status, reporting either no change[48] or a decrease in Akt phosphorylation.[49] Furthermore, Yeon et al[49] and Eo et al[50] did not observe any changes in phosphorylation for both mammalian target of rapamycin and p70S6k after Dex treatment of C2C12, which is consistent with our observations. Taken together, these findings suggest that Dex-induced skeletal muscle atrophy *in vitro* is a result of proteolytic degradation rather than the impairment of protein synthesis.

In conclusion, eEF2k/eEF2 cascade was shown to be dynamically regulated in response to disuse-associated muscle atrophy, with the onset of pathway perturbations occurring early during the HS period. An increase in $[Ca^{2+}]_i$ in skeletal muscle exposed to disuse, partially due to leakage of Cav1.1 channels, was sufficient to activate eEF2k, overcoming the inhibitory effect of S366 phosphorylation mediated by p70S6k. The present study provides evidence on the impact of the eEF2k/eEF2 pathway on p70S6k activity involved in translation initiation. Furthermore, increased phosphorylation status of eEF2 can down-regulate protein expression of atrophy biomarkers MAFbx/atrogin-1 and MuRF-1.

Supplemental Data

Supplemental material for this article can be found at *http://doi.org/10.1016/j.ajpath.2023.02.009*.

References

1. Fanzani A, Conraads VM, Penna F, Martinet W: Molecular and cellular mechanisms of skeletal muscle atrophy: an update. J Cachexia Sarcopenia Muscle 2012, 3:163−179
2. Gao Y, Arfat Y, Wang H, Goswami N: Muscle atrophy induced by mechanical unloading: mechanisms and potential countermeasures. Front Physiol 2018, 9:235
3. Phillips SM, Glover EI, Rennie MJ: Alterations of protein turnover underlying disuse atrophy in human skeletal muscle. J Appl Physiol (1985) 2009, 107:645−654
4. Baldwin KM, Haddad F, Pandorf CE, Roy RR, Edgerton VR: Alterations in muscle mass and contractile phenotype in response to unloading models: role of transcriptional/pretranslational mechanisms. Front Physiol 2013, 4:284
5. Gollnick PD, Piehl K, Saltin B: Selective glycogen depletion pattern in human muscle fibres after exercise of varying intensity and at varying pedalling rates. J Physiol 1974, 241:45−57
6. Edgerton VR, Roy RR: Neuromuscular adaptations to actual and simulated spaceflight. Edited by Fregly MJ, Blatteis CM. In Handbook of Physiology. Sect 4: Environmental Physiology. New York, NY: Oxford University Press, 1996. pp. 721−763
7. Mirzoev T, Tyganov S, Vilchinskaya N, Lomonosova Y, Shenkman B: Key markers of mTORC1-dependent and mTORC1-independent signaling pathways regulating protein synthesis in rat soleus muscle during early stages of hindlimb unloading. Cell Physiol Biochem 2016, 39:1011−1020
8. Stitt TN, Drujan D, Clarke BA, Panaro F, Timofeyva Y, Kline WO, Gonzalez M, Yancopoulos GD, Glass DJ: The IGF-1/PI3K/Akt pathway prevents expression of muscle atrophy-induced ubiquitin ligases by inhibiting FOXO transcription factors. Mol Cell 2004, 14: 395−403
9. Rhoads RE: Signal transduction pathways that regulate eukaryotic protein synthesis. J Biol Chem 1999, 274:30337−30340
10. Yoon MS: mTOR as a key regulator in maintaining skeletal muscle mass. Front Physiol 2017, 8:788
11. Ogasawara R, Fujita S, Hornberger TA, Kitaoka Y, Makanae Y, Nakazato K, Naokata I: The role of mTOR signalling in the regulation of skeletal muscle mass in a rodent model of resistance exercise. Sci Rep 2016, 6:31142
12. Cannavino J, Brocca L, Sandri M, Bottinelli R, Pellegrino MA: PGC1-alpha over-expression prevents metabolic alterations and soleus muscle atrophy in hindlimb unloaded mice. J Physiol 2014, 592: 4575−4589
13. Hornberger TA, Hunter RB, Kandarian SC, Esser KA: Regulation of translation factors during hindlimb unloading and denervation of skeletal muscle in rats. Am J Physiol Cell Physiol 2001, 281: 179−187
14. Wilson GJ, Moulton CJ, Garlick PJ, Anthony TG, Layman DK: Postmeal responses of elongation factor 2 (eEF2) and adenosine monophosphate-activated protein kinase (AMPK) to leucine and carbohydrate supplements for regulating protein synthesis duration and energy homeostasis in rat skeletal muscle. Nutrients 2012, 4: 1723−1739
15. Rose AJ, Alsted TJ, Jensen TE, Kobbero JB, Maarbjerg SJ, Jensen J, Richter EA: A Ca(2+)-calmodulin-eEF2K-eEF2 signalling cascade, but not AMPK, contributes to the suppression of skeletal muscle protein synthesis during contractions. J Physiol 2009, 587: 1547−1563
16. Browne GJ, Proud CG: Regulation of peptide-chain elongation in mammalian cells. Eur J Biochem 2002, 269:5360−5368
17. Ryazanov AG, Davydova EK: Mechanism of elongation factor 2 (EF-2) inactivation upon phosphorylation: phosphorylated EF-2 is unable to catalyze translocation. FEBS Lett 1989, 251:187−190
18. Pigott CR, Mikolajek H, Moore CE, Finn SJ, Phippen CW, Werner JM, Proud CG: Insights into the regulation of eukaryotic elongation factor 2 kinase and the interplay between its domains. Biochem J 2012, 442:105−118
19. Mitsui K, Brady M, Palfrey HC, Nairn AC: Purification and characterization of calmodulin-dependent protein kinase III from rabbit reticulocytes and rat pancreas. J Biol Chem 1993, 268:13422−13433
20. Wang X, Li W, Williams M, Terada N, Alessi DR, Proud CG: Regulation of elongation factor 2 kinase by p90(RSK1) and p70 S6 kinase. EMBO J 2001, 20:4370−4379
21. Shenkman BS, Nemirovskaya TL: Calcium-dependent signaling mechanisms and soleus fiber remodeling under gravitational unloading. J Muscle Res Cell Motil 2008, 29:221−230
22. Hofmann F, Flockerzi V, Kahl S, Wegener JW: L-type CaV1.2 calcium channels: from in vitro findings to in vivo function. Physiol Rev 2014, 94:303−326
23. Bodine SC, Latres E, Baumhueter S, Lai VK, Nunez L, Clarke BA, Poueymirou WT, Panaro FJ, Na E, Dharmarajan K, Pan ZQ, Valenzuela DM, DeChiara TM, Stitt TN, Yancopoulos GD, Glass DJ: Identification of ubiquitin ligases required for skeletal muscle atrophy. Science 2001, 294:1704−1708
24. Tischler ME, Rosenberg S, Satarug S, Henriksen EJ, Kirby CR, Tome M, Chase P: Different mechanisms of increased proteolysis in atrophy induced by denervation or unweighting of rat soleus muscle. Metabolism 1990, 39:756−763
25. Doig J, Griffiths LA, Peberdy D, Dharmasaroja P, Vera M, Davies FJ, Newbery HJ, Brownstein D, Abbott CM: In vivo characterization of the role of tissue-specific translation elongation factor 1A2 in protein synthesis reveals insights into muscle atrophy. FEBS J 2013, 280: 6528−6540
26. Schakman O, Kalista S, Barbe C, Loumaye A, Thissen JP: Glucocorticoid-induced skeletal muscle atrophy. Int J Biochem Cell Biol 2013, 45:2163−2172
27. Morey-Holton ER, Globus RK: Hindlimb unloading rodent model: technical aspects. J Appl Physiol (1985) 2002, 92:1367−1377
28. Xu Q, Yu L, Liu L, Cheung CF, Li X, Yee SP, Yang XJ, Wu Z: p38 Mitogen-activated protein kinase-, calcium-calmodulin-dependent protein kinase-, and calcineurin-mediated signaling pathways transcriptionally regulate myogenin expression. Mol Biol Cell 2002, 13: 1940−1952
29. Murphy RJ, Beliveau L, Gardiner PF, Calderone A: Nifedipine does not impede clenbuterol-stimulated muscle hypertrophy. Proc Soc Exp Biol Med 1999, 221:184−187
30. Goodman CA, Hornberger TA: Measuring protein synthesis with SUnSET: a valid alternative to traditional techniques? Exerc Sport Sci Rev 2013, 41:107−115
31. Pfaffl MW: A new mathematical model for relative quantification in real-time RT-PCR. Nucleic Acids Res 2001, 29:e45
32. Altaeva EG, Lysenko LA, Kantserova NP, Nemova NN, Shenkman BS: The basal calcium level in fibers of the rat soleus muscle under gravitational unloading: the mechanisms of its increase and the role in calpain activation. Dokl Biol Sci 2010, 433:241−243
33. Enns DL, Raastad T, Ugelstad I, Belcastro AN: Calpain/calpastatin activities and substrate depletion patterns during hindlimb unweighting and reweighting in skeletal muscle. Eur J Appl Physiol 2007, 100:445−455
34. Chen Z, Gopalakrishnan SM, Bui MH, Soni NB, Warrior U, Johnson EF, Donnelly JB, Glaser KB: 1-Benzyl-3-cetyl-2-methylimidazolium iodide (NH125) induces phosphorylation of eukaryotic elongation factor-2 (eEF2): a cautionary note on the anticancer mechanism of an eEF2 kinase inhibitor. J Biol Chem 2011, 286:43951−43958

35. Shahbazian D, Roux PP, Mieulet V, Cohen MS, Raught B, Taunton J, Hershey JW, Blenis J, Pende M, Sonenberg N: The mTOR/PI3K and MAPK pathways converge on eIF4B to control its phosphorylation and activity. EMBO J 2006, 25:2781−2791
36. Lecker SH, Solomon V, Mitch WE, Goldberg AL: Muscle protein breakdown and the critical role of the ubiquitin-proteasome pathway in normal and disease states. J Nutr 1999, 129:227S−237S
37. Massaccesi L, Goi G, Tringali C, Barassi A, Venerando B, Papini N: Dexamethasone-induced skeletal muscle atrophy increases O-GlcNAcylation in C2C12 Cells. J Cell Biochem 2016, 117: 1833−1842
38. Marzuca-Nassr GN, Vitzel KF, Murata GM, Marquez JL, Curi R: Experimental model of hindlimb suspension-induced skeletal muscle atrophy in rodents. Methods Mol Biol 2019, 1916:167−176
39. Ohira Y, Jiang B, Roy RR, Oganov V, Ilyina-Kakueva E, Marini JF, Edgerton VR: Rat soleus muscle fiber responses to 14 days of spaceflight and hindlimb suspension. J Appl Physiol (1985) 1992, 73: 51S−57S
40. Redpath NT, Proud CG: Purification and phosphorylation of elongation factor-2 kinase from rabbit reticulocytes. Eur J Biochem 1993, 212:511−520
41. Heise C, Gardoni F, Culotta L, di Luca M, Verpelli C, Sala C: Elongation factor-2 phosphorylation in dendrites and the regulation of dendritic mRNA translation in neurons. Front Cell Neurosci 2014, 8: 35
42. Sun Y, Caputo C, Edman KA: Effects of BAPTA on force and Ca2+ transient during isometric contraction of frog muscle fibers. Am J Physiol 1998, 275:C375−C381
43. Ito N, Ruegg UT, Kudo A, Miyagoe-Suzuki Y, Takeda S: Activation of calcium signaling through Trpv1 by nNOS and peroxynitrite as a key trigger of skeletal muscle hypertrophy. Nat Med 2013, 19: 101−106
44. Agrawal A, Suryakumar G, Rathor R: Role of defective Ca(2+) signaling in skeletal muscle weakness: pharmacological implications. J Cell Commun Signal 2018, 12:645−659
45. Nemirovskaya TL, Sharlo KA: Roles of ATP and SERCA in the regulation of calcium turnover in unloaded skeletal muscles: current view and future directions. Int J Mol Sci 2022, 23:6937
46. Pyr Dit Ruys S, Wang X, Smith EM, Herinckx G, Hussain N, Rider MH, Vertommen D, Proud CG: Identification of autophosphorylation sites in eukaryotic elongation factor-2 kinase. Biochem J 2012, 442:681−692
47. Csibi A, Cornille K, Leibovitch MP, Poupon A, Tintignac LA, Sanchez AM, Leibovitch SA: The translation regulatory subunit eIF3f controls the kinase-dependent mTOR signaling required for muscle differentiation and hypertrophy in mouse. PLoS One 2010, 5:e8994
48. Otsuka Y, Egawa K, Kanzaki N, Izumo T, Rogi T, Shibata H: Quercetin glycosides prevent dexamethasone-induced muscle atrophy in mice. Biochem Biophys Rep 2019, 18:100618
49. Yeon M, Choi H, Jun HS: Preventive effects of schisandrin A, a bioactive component of Schisandra chinensis, on dexamethasone-induced muscle atrophy. Nutrients 2020, 12:1255
50. Eo H, Reed CH, Valentine RJ: Imoxin prevents dexamethasone-induced promotion of muscle-specific E3 ubiquitin ligases and stimulates anabolic signaling in C2C12 myotubes. Biomed Pharmacother 2020, 128:110238